

Kinetics of the thermal decomposition of bis(dialkyldithiocarbamate) of palladium(II) complexes in isothermal and nonisothermal conditions

José Hilton G. Rangel, Severino Francisco Oliveira, José Geraldo P. Espínola,
Antonio Gouveia Souza*

Departamento de Química, CCEN, Universidade Federal da Paraíba, 58059-900, João Pessoa, Paraíba, Brazil

Accepted 17 November 1998

Abstract

Dialkyldithiocarbamate of palladium(II) complexes, $\text{Pd}(\text{S}_2\text{CNR}_2)_2$, with $\text{R}=\text{C}_2\text{H}_5$, $n\text{-C}_3\text{H}_7$, $n\text{-C}_4\text{H}_9$, $i\text{-C}_4\text{H}_9$ and C_5H_{11} were synthesized from the direct reaction of PdCl_2 with corresponding amine and carbon disulphide. The complexes were characterized by the techniques of melting points, infrared absorption spectroscopy and mass spectrometry.

The thermal decomposition reaction of complexes have been studied by isothermal and nonisothermal thermogravimetry. Superimposed curves of TG/DTG/DSC show that these reactions occur in the liquid phase. The kinetic isothermal model that best adjusted the experiment data were the R1 model. © 1999 Elsevier Science B.V. All rights reserved.

Keywords: Dialkyldithiocarbamate; Kinetics; Thermal decomposition; Palladium

1. Introduction

The research, to begin with, has been split mainly into general aspects and analytical applications of the compounds, in order to verify which of them, in the thermochemistry of metallic dithiocarbamates and similar compounds, have made a progressive development in the last decade [1–5].

There are other thermochemical data in literature, mainly with values for the standard molar enthalpies of formation and sublimation of different metal complexes of dithiocarbamates, essentially originating in the application of several techniques such as thermogravimetry, differential thermal analyser, differential scanning calorimetry, chromatography in phase gas, mass spectrometry and in smaller extension the calorimetry of solution and titration thermometrics [6].

Little investigation has been made concerning the kinetics of the thermal decomposition of the metallic complexes related to dithiocarbamates connected. Recently, Nunes and Machado [7,8] studied the kinetics of the isothermal and nonisothermal decomposition of the complexes $\text{Cd}(\text{S}_2\text{CNR}_2)_2$, where $\text{R}=\text{Et}$, Pr^n , Bu^n and Bu^i , a cross of the techniques of thermogravimetry (TG) and differential scanning calorimetry (DSC), concluding that there is no direct relation between activation energy determined and the thermal stability of the complexes.

2. Experimental

2.1. Chemicals

The solvents used in all preparations were distilled and stored over Linde 4A molecular sieves. Diethylamine, di-*n*-propylamine, di-*n*-butylamine, di-iso-

*Corresponding author. Fax: +55-83-216-7441; e-mail: gouveia@quimica.ufpb.br

butylamine and di-*n*-pentylamine (Merck) and carbon disulphide (Merck) were distilled, respectively. The palladium(II) chloride (Merck) was dried in vacuo.

2.2. Preparations

The dialkyldithiocarbamate of palladium(II) complexes $[\text{Pd}(\text{S}_2\text{CNR}_2)_2]$, with $\text{R}=\text{C}_2\text{H}_5$, *n*- C_3H_7 , *n*- C_4H_9 , *i*- C_4H_9 and C_5H_{11} were synthesized from the direct reaction of PdCl_2 with corresponding amine and carbon disulphide in acetone. After filtration, the crystals formed were recrystallized from ethanol and dried in vacuo, with yields in the range 82–85%. The complexes obtained were stored in a desiccator over calcium chloride. Microanalysis for carbon, hydrogen and nitrogen were within experimental error of the expected values from the established formulas.

2.3. Thermal measurements

Thermogravimetric curves were obtained using a Shimadzu model TGA-50 thermobalance, under nitrogen atmosphere, by isothermal and nonisothermal heating techniques. The carrier gas flow was always 0.83 ml s^{-1} , the sample mass was $5.0 \pm 0.5 \text{ mg}$ and the heating rate was 10 K min^{-1} for the isothermal.

The DSC curves were obtained in nitrogen atmosphere, using a differential scanning calorimeter Shimadzu model DSC-50, with heating rate of 10 K min^{-1} .

2.4. Other measurements

The melting temperatures for all compounds were determined by means of a Microquímica

model MQAPF-301 apparatus. Infrared spectra were recorded as KBr pellets, in the region $4000\text{--}4400 \text{ cm}^{-1}$ using a Bomem model MB-102 series FTIR spectrophotometer, mass spectra of the ligand and chelates on a Hewlett-Packard model 5988A spectrometer with an ionization energy of 70 eV, at 523 K.

The nonisothermal parameter kinetics of the $\text{Pd}(\text{S}_2\text{CNR}_2)_2$ complexes was determined by Coats–Redfern [9] method in VISUAL BASIC program developed in TAL (Thermal Analysis Laboratory). A VISUAL BASIC program (for linear regression) was also developed in TAL for the isothermal method.

3. Results and discussion

The CHN elemental analysis of the complexes, $[\text{Pd}(\text{S}_2\text{CNR}_2)_2]$, with $\text{R}=\text{C}_2\text{H}_5$, *n*- C_3H_7 , *n*- C_4H_9 , *i*- C_4H_9 and *n*- C_5H_{11} , are in good agreement with the expected values for compounds as shown in Table 1. The behaviour of both complexes on heating is very similar. The melting temperature observed is well defined, as indicated in Table 1, which also lists the decomposition temperature range for the thermogravimetric determinations. The mode of coordination of the dialkyldithiocarbamate and the definite melting points suggest the existence of very stable compounds. The samples in the study were not submitted to be controlled granulometrically, because, all the complexes are decomposed to a temperature above the respective melting temperatures, as shown in Fig. 1 (a) and (b), in the curves TG/DTG/DSC for the complex $\text{Pd}(\text{S}_2\text{CNPr}_2)_2$.

The νCN band assumes a double-band character which is reflected in the appearance of a stretching

Table 1
Melting points (K), TG temperature interval of the isothermal decomposition (K), main absorptions in the infrared (cm^{-1}) and mass percentage analyses (%) for complexes

Complexes	Melting point	Temperature interval	$\nu(\text{C-S})$	$\nu(\text{C=N})$	C		N		H	
					T	P	T	P	T	P
$\text{Pd}(\text{S}_2\text{CNEt}_2)_3$	518	541–561	987.66	1518.91	29.80	29.81	6.96	6.97	5.01	4.86
$\text{Pd}(\text{S}_2\text{CNPr}_2)_3$	423	568–588	970.43	1513.49	36.63		6.10		6.16	
$\text{Pd}(\text{S}_2\text{CNBu}_2)_3$	385	561–586	965.74	1509.23	41.96	42.93	5.44	5.50	7.06	7.11
$\text{Pd}(\text{S}_2\text{CNBu}_7)_3$	465	535–546	979.55	1503.64	41.96	42.57	5.44	5.48	7.06	6.92
$\text{Pd}(\text{S}_2\text{CNPe}_2)_3$	381	573–598	964.69	1511.62	46.21	46.33	4.90	4.90	7.78	7.91

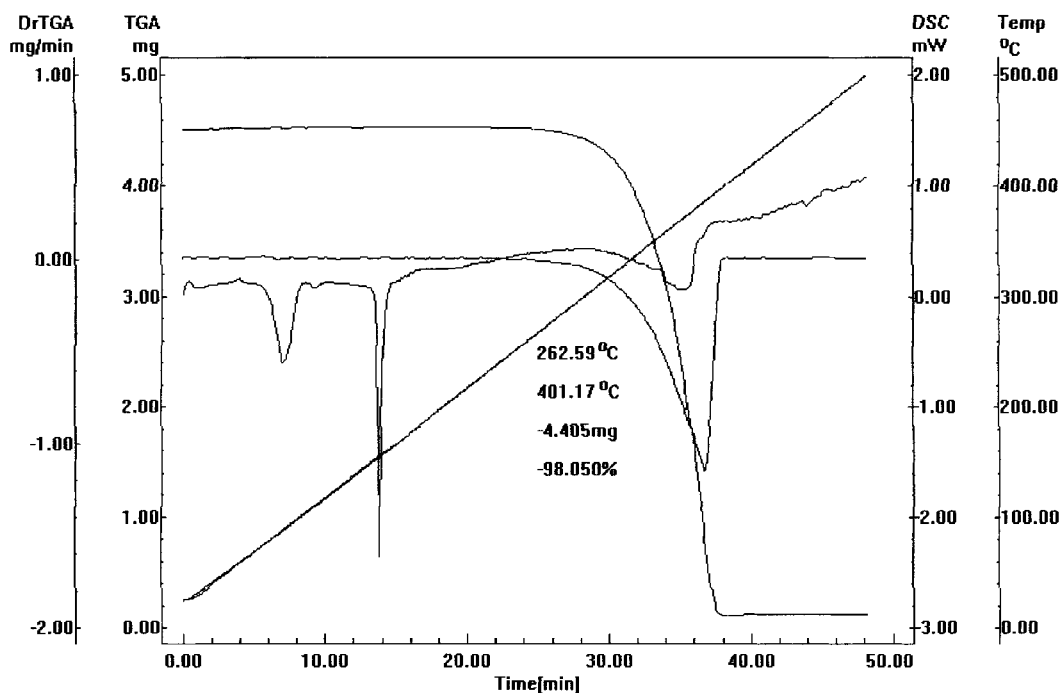


Fig. 1. TG/DTG/DSC plots of the $\text{Pd}(\text{S}_2\text{CNPr}_2)_2$.

band shifted to higher frequency. For all complexes this band frequency is higher than that of the respective ligand. On the other hand, a decrease in the νCS stretching band is observed and an isolated band near 1000 cm^{-1} indicates that the ligand is bonded to metal in a bidentate manner [10]. The principal infrared bands observed are listed in Table 1. The mass spectra of the complexes revealed the presence of the parent ions with the following order of stability: $\text{Pd}(\text{S}_2\text{CNPr}_2)_2 > \text{Pd}(\text{S}_2\text{CNBu}_2)_2 > \text{Pd}(\text{S}_2\text{CNPe}_2)_2 > \text{Pd}(\text{S}_2\text{CNEt}_2)_2 > \text{Pd}(\text{S}_2\text{CNBu}_2)_2$. The principal fragments observed in the mass spectra for the complexes are shown in Table 2.

The application of the isothermal method in thermal decomposition study of reactions of complexes enables us to identify the mechanism for which the reaction is processed, as well as to determine the parameter kinetics, apparent activation energy, E , and frequency factor, A .

The choice of the temperature adopted to the accomplishment of the experiment was made with the help of the curve TG dynamics, by heating to

$10^\circ\text{C min}^{-1}$ the temperature intervals observed in Table 1 enables us to identify the mechanism for which the reaction is processed, as well as to determine the parameter kinetics, apparent activation energy, E , and frequency factor, A .

Did the identification of the mechanism adopted in the process occur based on different models of the heterogeneous reactions in the solid state [11]? The results for $\text{Pd}(\text{S}_2\text{CNEt}_2)_2$ are listed in Table 3. The experimental data treated by techniques of linear regression are obtained by using the relationship $g(\alpha) = kt + k_0$. Adjustments were made for values of the decomposed function, α , greater than 0.15 as the experience of not presenting the characteristic isothermal begins attenuating the incidence of mistakes.

Using an interval $0.15 < \alpha < 0.95$, and on the basis of the best adjustment of the coefficient of linear correlation the models R1 and A4 presented better results, as shown in Table 3, and are listed in Table 4. In Fig. 2 we can define with larger precision as to which of the two models represents the process better.

Table 2
Principal fragments of mass observed for complexes

Fragments	Pd(S ₂ CNEt ₂) ₂		Pd(S ₂ CNPr ⁿ) ₂		Pd(S ₂ CNBu ⁿ) ₂		Pd(S ₂ CNBu ⁱ) ₂		Pd(S ₂ CNPe ⁿ) ₂	
	<i>m/e</i>	<i>I</i> (%)	<i>m/e</i>	<i>I</i> (%)	<i>m/e</i>	<i>I</i> (%)	<i>m/e</i>	<i>I</i> (%)	<i>m/e</i>	<i>I</i> (%)
[ML ₂] ⁺	402.95	11.93	459.10	31.50	515.20	13.94	515.25	9.63	571.40	13.10
[ML] ⁺	254.90	30.12	282.74	46.00	311.00	15.00	310.95	19.71	339.00	10.91
[L] ⁺	148.80	3.76	176.34	4.00	204.95	3.28	205.00	3.24	232.96	6.31
[R ₂ NCS] ⁺	116.00	44.51	144.28	25.50	172.00	31.81	171.95	18.51	200.90	6.54
[RNHCS] ⁺	88.05	52.05	102.19	23.00	116.00	30.02	116.05	15.14	162.00	2.68
[R ₂ N] ⁺	72.05	100.00	100.21	69.00	128.15	100.00	128.05	28.03	156.15	78.68
[RNCH] ⁺	56.15	9.74	70.13	7.50	84.05	7.43	84.15	6.56	130.05	19.30
[H ₂ NCS] ⁺	60.00	45.00	60.10	13.50	60.00	14.46	60.05	8.22	60.05	8.94
[RNCS] ⁺	–	–	101.18	1.50	115.15	1.71	114.95	1.69	161.00	5.02
[R] ⁺	29.20	24.34	–	–	57.15	72.86	57.20	89.56	71.20	40.80

Table 3
Linear correlation coefficients (*r*) and standard deviation (sd) of the Pd(S₂CNEt₂)₂ in the temperature range 541–561 K

Temperature	Parameter	Model			
		R1	A2	A3	A4
541	<i>r</i>	0.9999	0.9899	0.9958	0.9972
	sd	3.25 × 10 ⁻³	4.82 × 10 ⁻²	2.11 × 10 ⁻²	1.30 × 10 ⁻²
545	<i>r</i>	0.9999	0.9895	0.9957	0.9974
	sd	2.46 × 10 ⁻³	4.96 × 10 ⁻²	2.14 × 10 ⁻¹	1.28 × 10 ⁻²
557	<i>r</i>	0.9999	0.9886	0.9952	0.9971
	sd	8.59 × 10 ⁻⁴	5.17 × 10 ⁻²	2.27 × 10 ⁻²	1.35 × 10 ⁻²
559	<i>r</i>	0.9999	0.9884	0.9950	0.9969
	sd	8.59 × 10 ⁻³	5.15 × 10 ⁻²	2.29 × 10 ⁻²	1.39 × 10 ⁻²
561	<i>r</i>	0.9999	0.9875	0.9945	0.9965
	sd	1.82 × 10 ⁻³	5.35 × 10 ⁻²	2.41 × 10 ⁻²	1.46 × 10 ⁻²

The parameter *k*₀ of the equation of speed was approximately equal to naught in every fitting, justified by the fact of the experimental curve, Fig. 1, practically not to present induction period in its beginning.

The integral methods are habitually the favourites because they do not present the disadvantage of dispersion of the data that frequently hinders or disables the use of the methods you differentiate [12–15]. However, when used they should be used with caution, because almost always meet a group of kinetic parameters (*E*, *A*, and *n*) adapted to the experimental data, and these parameters contribute to the understanding of the mechanism of the studied reaction [14].

The method of Coats–Redfern [9] was used for $\phi=10 \text{ K min}^{-1}$, with the substitution of the functions *g*(α) to give

$$\ln \left[\frac{g(\alpha)}{T^2} \right] = \ln \left[\frac{AR}{\phi E} \right] - \frac{E}{RT}.$$

In spite of the ease in the application of the non-isothermal methods in relation to the isothermal, this last one presents more reliable results, serving besides as reference in the comparison of the parameters obtained through dynamic method.

The parameter kinetic activation energy, *E*, and frequency factor, *A*, were certain through the equation of Arrhenius with the constants of speed, *k*, relative to

Table 4
Linear correlation coefficients (r) and standard deviation (sd) of the complexes in each range of temperature

Complexes	Temperature (K)	Parameter	Model	
			R1	A4
Pd(S ₂ CNEt ₂) ₂	541	r	0.9999	0.9972
		sd	3.25×10^{-3}	1.30×10^{-2}
	545	r	0.9999	0.9974
		sd	2.46×10^{-3}	1.28×10^{-2}
	557	r	0.9999	0.9971
		sd	8.59×10^{-4}	1.35×10^{-2}
	559	r	0.9999	0.9969
		sd	8.59×10^{-3}	1.39×10^{-2}
	561	r	0.9999	0.9965
		sd	1.82×10^{-3}	1.46×10^{-2}
Pd(S ₂ CNPr ⁿ) ₂	568	r	0.9999	0.9973
		sd	3.77×10^{-3}	1.31×10^{-2}
	573	r	0.9999	0.9967
		sd	1.43×10^{-3}	1.40×10^{-2}
	578	r	0.9999	0.9969
		sd	8.01×10^{-4}	1.38×10^{-2}
	583	r	0.9999	0.9971
		sd	3.27×10^{-3}	1.32×10^{-2}
	588	r	0.9995	0.9976
		sd	7.67×10^{-3}	1.22×10^{-2}
Pd(S ₂ CNBu ⁿ) ₂	561	r	0.9999	0.9972
		sd	2.41×10^{-3}	1.30×10^{-2}
	571	r	0.9999	0.9974
		sd	2.56×10^{-3}	1.27×10^{-2}
	576	r	0.9999	0.9975
		sd	2.34×10^{-3}	1.26×10^{-2}
	581	r	0.9999	0.9971
		sd	1.27×10^{-3}	1.32×10^{-2}
	586	r	0.9999	0.9971
		sd	1.10×10^{-3}	1.34×10^{-2}
Pd(S ₂ CNBu ⁱ) ₂	535	r	0.9999	0.9975
		sd	3.49×10^{-3}	1.24×10^{-2}
	538	r	0.9998	0.9975
		sd	3.89×10^{-3}	1.25×10^{-2}
	541	r	0.9997	0.9979
		sd	5.97×10^{-3}	1.14×10^{-2}
	543	r	0.9998	0.9978
		sd	4.52×10^{-3}	1.10×10^{-1}
	546	r	0.9994	0.9984
		sd	8.48×10^{-3}	1.01×10^{-2}
Pd(S ₂ CNPe ⁿ) ₂	573	r	0.9999	0.9969
		sd	9.44×10^{-4}	1.36×10^{-2}
	578	r	0.9999	0.9969
		sd	6.92×10^{-4}	1.38×10^{-2}
	588	r	0.9999	0.9973
		sd	2.41×10^{-3}	1.29×10^{-2}
	593	r	0.9999	0.9966
		sd	2.09×10^{-3}	1.43×10^{-2}
	598	r	0.9999	0.9971
		sd	1.44×10^{-3}	1.34×10^{-2}

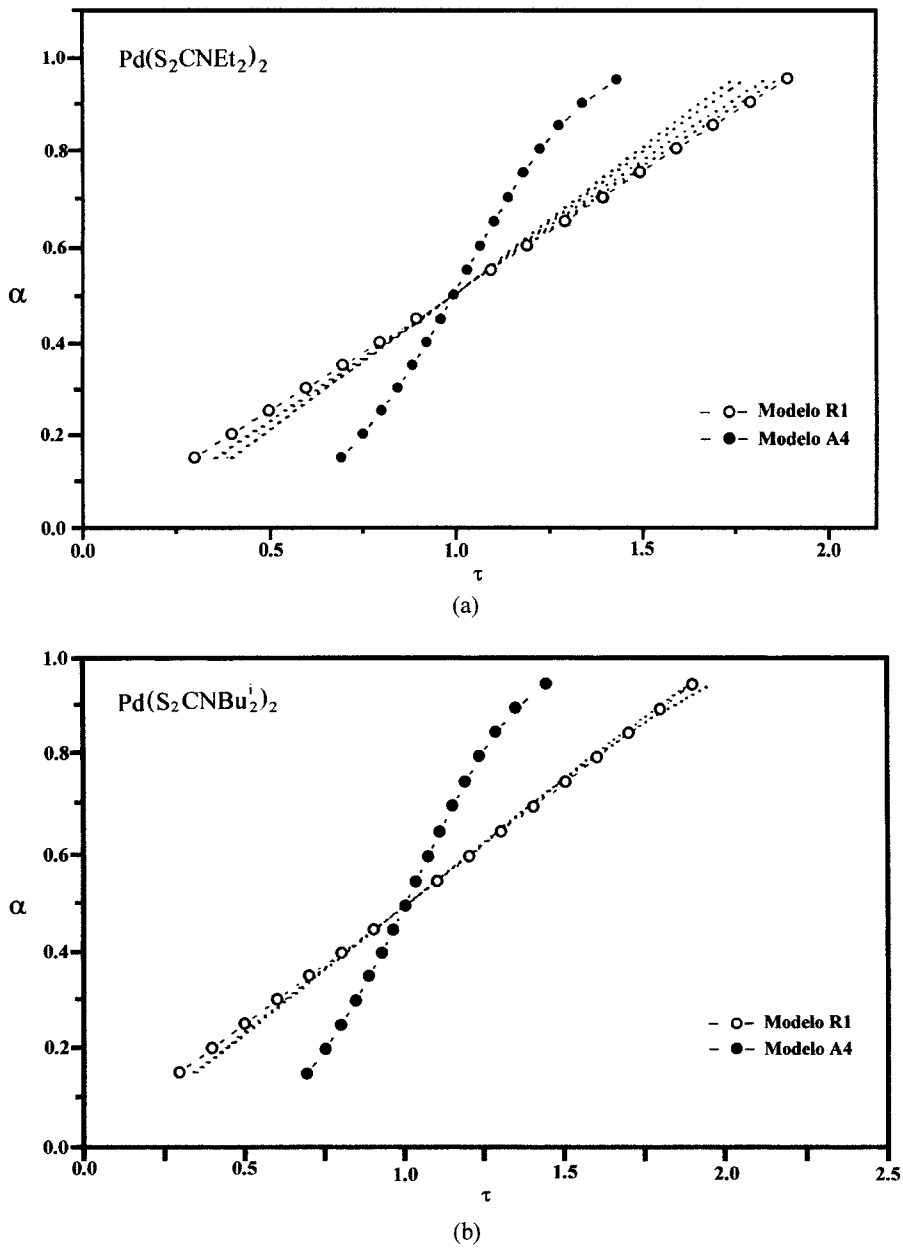


Fig. 2. Reduced plot for the isothermal decomposition of (a) $\text{Pd}(\text{S}_2\text{CNEt}_2)_2$ and (b) $\text{Pd}(\text{S}_2\text{CNBu}_2)_2$ using R1 and A4 models.

the model R1 as exhibition of the example for the $\text{Pd}(\text{S}_2\text{CNBu}_2)_2$ of Fig. 3.

The models found by the nonisothermal method, Table 5, are in agreement with those observed for the

isothermal method, Table 6. However, it would be very difficult to identify the model for this method without confronting the results with that of the isothermal one.

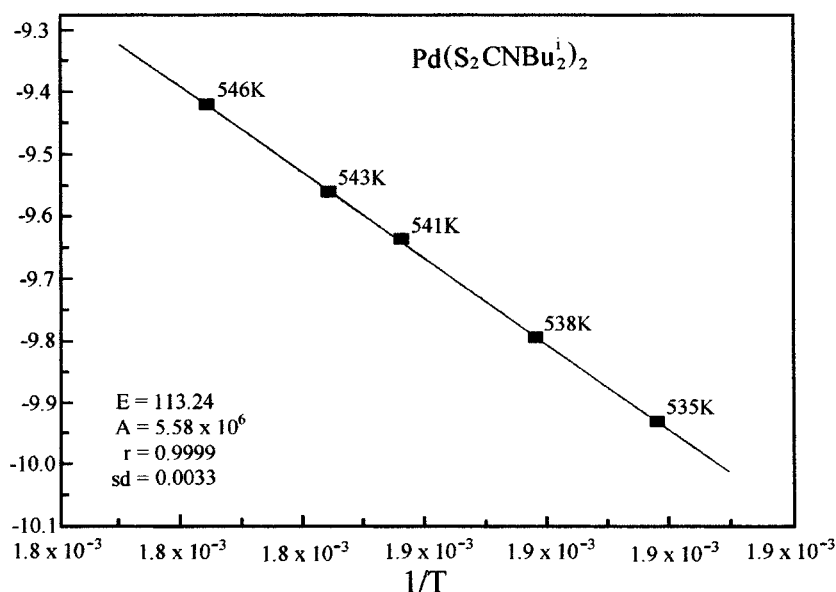


Fig. 3. Adjustment of the graph using the model R1 in the determination of the kinetic parameters for isothermal thermogravimetry, according to the law of Arrhenius for $\text{Pd}(\text{S}_2\text{CNBu}_2)_2$.

Table 5

Kinetic parameters derived from isothermal thermogravimetry for application of the Arrhenius law using the R1 model

Parameters	Complex				
	$\text{Pd}(\text{S}_2\text{CNEt}_2)_2$	$\text{Pd}(\text{S}_2\text{CNPr}_2)_2$	$\text{Pd}(\text{S}_2\text{CNBu}_2)_2$	$\text{Pd}(\text{S}_2\text{CNBu}_2)_2^i$	$\text{Pd}(\text{S}_2\text{CNPe}_2)_2$
E (kJ mol^{-1})	112.43	116.17	135.05	112.44	134.58
A (s^{-1})	4.89×10^6	7.51×10^6	1.63×10^8	5.58×10^6	8.43×10^7
r	0.9984	0.9656	0.9979	0.9999	0.9998
sd	0.0266	0.103	0.0363	0.0033	0.0102

Table 6

Kinetic parameters derived from application of the function $g(\alpha)$ in the Coats–Redfern equation (5) for $\phi=10 \text{ K min}^{-1}$, E (kJ mol^{-1}) and A (s^{-1})

Complex	Parameter	Model			
		A3	A4	R1	R2
$\text{Pd}(\text{S}_2\text{CNEt}_2)_2$	E	44.72	30.92	104.42	127.07
	A	9.43	4.92×10^{-1}	9.37×10^5	5.05×10^7
	r	0.9846	0.9821	0.9997	0.9978
$\text{Pd}(\text{S}_2\text{CNPr}_2)_2$	E	39.46	27.02	121.22	129.92
	A	2.71	1.87×10^{-1}	2.21×10^7	6.80×10^7
	r	0.9999	0.9999	0.9999	0.9999
$\text{Pd}(\text{S}_2\text{CNBu}_2)_2$	E	70.14	46.90	157.93	191.46
	A	1.13×10^3	2.02×10^1	1.30×10^{10}	5.87×10^{12}
	r	0.9679	0.9646	0.9935	0.9917
$\text{Pd}(\text{S}_2\text{CNBu}_2)_2^i$	E	34.80	23.48	83.67	102.34
	A	1.12	9.14×10^{-2}	1.48×10^4	3.77×10^5
	r	0.9896	0.9874	0.9981	0.9991
$\text{Pd}(\text{S}_2\text{CNPe}_2)_2$	E	123.97	90.25	264.45	321.20
	A	3.19×10^7	5.16×10^4	4.30×10^{18}	9.88×10^{22}
	r	0.9357	0.9322	0.9694	0.9577

Acknowledgements

The authors thank CAPES, CNPq and PADCT for the scholarship and financial support for the accomplishment of this work.

References

- [1] D. Coucouvanis, *Prog. Inorg. Chem.* 11 (1970) 233.
- [2] R.J. Magee, *Rev. Anal. Chem.* 1 (1973) 333.
- [3] A.G. Souza, F. Souza Neto, J.H. Souza, R.O. Macêdo, J.B.L. Oliveira, C.D. Pinheiro, *J. Thermal Anal.* 49 (1997) 679.
- [4] A.G. Souza, C.D. Pinheiro, L.C./R. Santos, M.L.M. Melo, *Thermochim. Acta* 231 (1994) 31.
- [5] J.O. Hill, R.J. Magee, *Rev. Inorg. Chem.* 3 (1981) 141.
- [6] M.I. Yoshida, M.M. Braga, J.C. Machado, *Thermochim. Acta* 237 (1994) 347.
- [7] L.M. Nunes, *Cinetica de Termodecomposição de Complexos Dialquilditiocarbamato Cádmio(II)*, Dissertação de Mestrado, UFPB, João Pessoa, PB, Brazil, 1995.
- [8] M.C.N. Machado, *Estudo Cinético da Termodecomposição de Complexos Bis(dialquilditiocarbamato) Cd(II) por Termogravimetria Dinâmica e Isotérmica*, Dissertação de Mestrado, UFPB, João Pessoa, PB, Brazil, 1996.
- [9] A.W. Coats, J.P. Redfern, *Nature* 201 (1964) 68.
- [10] F. Bonati, R. Ugo, *J. Organomet. Chem.* 10 (1967) 257.
- [11] M.I. Yoshida, *Cinética e Mecanismo de Reação de Decomposição Térmica no Estado Sólido: Influência de Variações Estruturais no Ligante, Sobre os Parâmetros Cinéticos*, Tese de Doutorado, Instituto de Ciências Exatas, Universidade Federal de Minas Gerais, Belo Horizonte, MG, Brazil, 1995.
- [12] T. Ozawa, *J. Thermal Anal.* 2 (1970) 301.
- [13] J.H. Flynn, L.A. Wall, *J. Res. Natl. Bur. Stand.* 70A(6) (1966) 487.
- [14] J. Sestak, *J. Thermal Anal.* 16(2) (1979) 503.
- [15] J. Zsacó, *J. Thermal Anal.* 5(2) (1973) 239.